Evolution of Ni_3X Precipitation Kinetics, Morphology and Spatial Correlations in Binary Ni-X Alloys Aged Under Externally Applied Stress

Final Report

Covering the Grant Period
June 15, 1999 to October 31, 2004

Alan J. Ardell, Principal Investigator
Department of Materials Science and Engineering
University of California
Los Angeles, CA 90095-1595

Grant # DE-FG03-96ER45573

January 31, 2006

I. Personnel

During the lifetime of the project the following personnel were employed:

Yong Ma, graduate student, Department of Materials Science and Engineering, worked for about a year before switching to another project;

Natalia Starostina, best described as a post-masters researcher without a graduate degree objective, Department of Materials Science and Engineering, worked on the project for about 2 years before leaving for a full-time job;

Mark Opoku-Adusei, postdoctoral researcher, Department of Materials Science and Engineering, was partly supported by the project for about a year before taking a full-time job;

Suman Prasad, graduate student, Department of Materials Science and Engineering, worked for less than a year before leaving UCLA

J.D. Carnes, graduate student, Department of Earth and Space Sciences and Institute of Geophysics and Planetary Physics, worked for a few months during 2 summers;

Steve Moser, graduate student, Department of Earth and Space Sciences and Institute of Geophysics and Planetary Physics, worked for a few months during 1 summer;

Deborah Detch, graduate student, Department of Materials Science and Engineering, worked for about a year before leaving the project;

Roberto Guerrero, postdoctoral researcher, Department of Materials Science and Engineering, was supported by the project for about 2 years until it ended;

Sergey V. Prikhodko, collaborator, Department of Materials Science and Engineering, worked in this capacity at no charge for the lifetime of the project;

Donald G. Isaak, collaborator, Institute of Geophysics and Planetary Physics, UCLA, and Professor, Department of Math and Physics, Azusa Pacific University, worked on the project during the summers.

II. Publications

1. S.V. Prikhodko, D.G. Isaak, J.D. Carnes, S. Moser, Y. Ma, and A.J. Ardell "Elastic Constants of FCC and $L1_2$ Ni-Si Alloys: Composition and Temperature Dependence", *Metallurgical and Materials Transactions A* 34A (2003) 1863-1868.
2. S.V. Prikhodko and A.J. Ardell, "Coarsening of γ' in Ni-Al Alloys Aged Under Uniaxial Compression: I. Early-Stage Kinetics", *Acta Materialia* 51 (2003) 5001-5012.
3. A.J. Ardell and S.V. Prikhodko, " Coarsening of γ' in Ni-Al Alloys Aged Under Uniaxial Compression: II. Diffusion Under Stress and Retardation of Coarsening Kinetics *Acta Materialia* 51 (2003) 5013-5019.
4. S.V. Prikhodko and A.J. Ardell, "Coarsening of γ' in Ni-Al Alloys Aged Under Uniaxial Compression: III. Characterization of the Morphology", *Acta Materialia* 51 (2003) 5021-5036.

5. N.V. Starostina, S.V. Prikhodko, A.J. Ardell and S. Prasad, "Coarsening of Ni_3Ge Precipitates in Ni-Ge Alloys Aged under Uniaxial Compression", *Materials Science and Engineering A*, **397** (2005) 264-270.

6. S.V. Prikhodko, D.G. Isaak, E. Fisher, N.V. Starostina, Y. Ma and A.J. Ardell, "The Elastic Constants of FCC Ni-Ga and Ni-Ge Alloys up to 1100 K", *Scripta Materialia*, accepted for publication.

III. Presentations

S.V. Prikhodko and A.J. Ardell, "Coarsening Kinetics and Morphology of Ni_3Al Precipitates in Alloys Aged Under Uniaxial Compression", 2000 TMS Fall Meeting, St. Louis, MO, October 2000.

N.V. Starostina and A.J. Ardell, "Coarsening of Ni_3Ge Precipitates Under Uniaxial Compression", TMS 2001, New Orleans, LA, February 2001.

IV. Research

IV.1 Ni-Al Single Crystals Aged Under Compression (S.V. Prikhodko)

The results of this research were published in papers #2 and 4, Sec. II. A summary of the main results follows.

Experiments were performed on cylindrically symmetric specimens with the axis of the applied compressive stress parallel to [100]. The geometries employed included doubly tapered (DT) specimens ~10 mm long with diameters varying from ~ 3 to 6 mm and right cylindrical (RC) specimens ~4 mm in diameter and ~3 mm in length. The DT geometry was chosen because microstructural evolution under stress could be investigated without requiring a unique specimen for each stress. We chose to vary the diameter of the cross section by factor of approximately 2, so that the stress varied by about factor of 4. The experiments on the RC specimens were done, in part, to evaluate the possible effects of the stress gradient that is always present in the DT samples. The state of stress is multiaxial near the periphery of the DT specimens, but the microstructures were examined near the axis of each specimen where the stress is uniaxial.

A single crystal Ni-Al alloy ~25 mm in diameter and 80 mm long, grown by the Bridgman method, was purchased from Alloy Preparation Facility of the Ames Laboratory (Ames, IA). The nominal composition of the alloy was 13.36 at. % Al, but during solidification some variation of the Al concentration along the entire length of the bulk crystal is inevitable. Since the partition coefficient in the Ni-Al system is not much greater than unity, the segregation of Al was relatively small, amounting to ~1.8 at. % over most of the useable length of the crystal (~35 mm). The variation in concentration was determined by measuring the ferromagnetic Curie temperature, Θ_C, of small pieces of the alloy taken from slices along the length of the single crystal; reference to an established calibration curve of Θ_c vs. Al concentration was used for this purpose. The concentration of Al in the DT specimens varied from 12.5 to 13.5 % Al; in the RC specimens the concentration varied from 13.7 to 14.1 %.

The single crystal was homogenized at 1200 °C for 72 h. Laue back-reflection x-ray diffraction was used to orient the bulk crystal, a low-speed diamond wheel was used to slice it and a lathe was used to machine the DT and RC specimens to their final dimensions. The orientation of the specimens deviated from [100] by no more than 2°. The specimens were solution treated in an Ar atmosphere at 1200 °C for 0.5 h, followed by quenching in refrigerated brine.

A stainless steel fixture was used for aging the specimens under compressive load. The load was applied through a lever arm with a calibrated lever ratio, and transferred to the specimen via tensile linkage. A dual-elliptical infrared reflector furnace was used for heating. This furnace enabled the specimen to be heated and cooled at fairly rapid rates. The heating rate from room temperature was ~1.2 °C/s to 640 °C, while the cooling rate from 640 to 500 °C was ~1 °C/s; below 500 °C the kinetics of decomposition of the supersaturated matrix are too slow to affect the microstructure. The temperature was controlled to within ±1 °C, and long-time stability of the temperature was measured to be ±1.5 °C over a period of 24 h. A protective Ar atmosphere helped to minimize oxidation of the specimens and fixture during testing. The reference and control thermocouples were initially calibrated using a third one, which was welded directly to a dummy sample having the same DT configuration as those tested. The temperature calibration was checked periodically throughout the course of the research project. The advantages of rapid heating and cooling in the radiant heating furnace are partially offset by uncertainties in the precise temperatures of the specimens. Small variations in temperature can arise owing to the small thermal mass of the furnace, rendering the temperature susceptible to uncertainties that are difficult to control. The intimacy of contact between the surfaces of the specimens and the loading fixture is an example; it can be expected to differ somewhat for loaded and unloaded specimens. The length of the specimens is another factor. The main point is that small excursions in temperature can have a considerable effect on the kinetics, and we believe that this was responsible for much of the scatter in the data.

All the samples were aged at a nominal temperature of 640 °C. At this temperature the volume fraction of γ′ in the alloy was ~10-15% for the DT specimens and 18-20% for the RC specimens. The DT specimens were aged for 10, 24, 72, 120 (two samples), 310, 504 and 1021 h under a single applied load of 940 N. The applied stress in the tapered specimens varied from ~30 to ~130 MPa; the stress gradient was ~18 MPa/mm. Unstressed reference specimens were aged together with stressed ones. All the RC samples were aged for 120 h under stresses in the range 0 to 150 MPa. To minimize plastic deformation of the RC specimen aged under the biggest applied stress used (151 MPa), it was aged first for 5 h at a lower stress (~112 MPa) after which the additional load was added. After aging, the specimens were examined for plastic deformation by checking their dimensions. Even for the longest aging time plastic deformation amounted to less than 4% in the narrowest part of the tapered samples. In most of the experiments on the stressed specimens a reference sheet specimen was placed alongside the DT or RC specimen and used as controls, particularly on the aging temperature. Examination of these specimens consistently produced smaller γ′ precipitates than expected by comparison with results in the literature. We believe this was a consequence of the lack of complete uniformity of the temperature in the fixture, especially for samples that were not in intimate contact with the fixture itself and off-center at the same time, thereby experiencing lower temperatures than expected.

The microstructures of all the specimens were evaluated using transmission electron microscopy (TEM). Thin foils were prepared by slicing the samples in a direction perpendicular to the axis of the applied stress. For comparison a few specimens were cut parallel to (100), i.e. parallel to the applied stress. The slices were ground to ~300 mm and their diameters were measured using a Sherr Tumico bench top horizontal optical comparator for calculating the applied stresses from the known load. Disks 3 mm in diameter were punched from the slices and ground to a thickness of ~150 mm. TEM samples were prepared by dimpling the discs electrochemically using a solution of 20% HNO_3, 15% CH_3COOH, 20% H_3PO_4 and 45% H_2O, at 60 V, followed by electrochemical polishing at 20 V using a solution of 20% H_2SO_4 and 80% CH_3OH at room temperature.

TEM examination was done using a JEOL model 100 CX TEMSCAN electron microscope operating at an accelerating voltage of 100 kV. Dark-field images of the precipitates were

taken using a {100} superlattice reflection from the ordered γ'-phase. All the specimens had natural orientations close to ⟨100⟩ so almost no tilting was necessary. The radius of an individual particle was calculated from the formula $r = r_{min}(A + 1)/2$, where r_{min} is the radius of the smallest circle inscribed in the image of the particle and A is the aspect ratio of the particle. Between 300 and 600 particles were measured for each condition. For the initial stages of the project we decided to photograph all the images at a magnification of 20,000. This facilitated the comparison of the precipitate microstructures as a function of σ, as well as from one aging time to the next. Unfortunately, the errors associated with the characterization of the shapes of individual precipitates can be large, depending on their sizes relative to the magnification at which they are photographed. For this reason, reliable data on the shapes were obtained only for the larger particles. After examination in the TEM many of the specimens were re-solution treated for the purpose of measuring Θ_c. This helped to establish the overall Al concentration of the specimen and check the concentration gradient along a single compression sample. However, the minor oxidation during heat-treatment completely obviated their re-examination in the TEM.

The exposure time of a TEM negative can significantly affect the apparent sizes of the γ' precipitates. This is evident on exposing the same area of the thin foil for different times which all yield satisfactory images. Under these conditions the measured particle sizes increase with increasing exposure time. Since different thin foil specimens will always be slightly different in thickness and orientation, the background level will differ from one dark-field image to the next. We tried to find a reliable method for compensating for different background gray levels in different negatives, but were unsuccessful. Therefore very effort was made to ensure that the background densities in all the negatives were equal. While this appears to be the case in nearly all the photographs taken, the task is truly impossible and introduced yet another source of error into the measurements.

We found that compressive stress retards the kinetics of coarsening by 20 to 25% at 150 MPa. The particle size distributions become broader as the stress increases. We attribute the slower kinetics under compressive stress to its effect on the coefficient of diffusion of Al. An elasticity-based model was developed for predicting how the coefficient of diffusion, D, changes under an applied compressive stress (paper #3, Sec. II). Stress affects the activation energy for motion, Q_M, of an atom, as well as its jump distance, ℓ. Since a cubic crystal is slightly distorted tetragonally under uniaxial stress, Q_M and ℓ, hence D, both become different in directions normal and parallel to the stress axis. Q_M was calculated using a dynamical model of diffusion due to Flynn. Using the elastic constants for Ni-Al alloys, and taking into account the effect of the hydrostatic component of the applied stress on D, the model predicts that D decreases by about 6 % under an applied stress of 150 MPa. This reduction did not account entirely for the retardation of coarsening kinetics observed experimentally, but given the simplicity of the model the result was considered satisfactory.

The aspect ratio, A, of a γ' precipitate, as well as a shape parameter, Σ, which provides a measure of how cuboidal it is, were used to characterize the γ' morphology. Σ is defined by the equation

$$\Sigma = \frac{S_p - S_4}{0.5708\, S_4}, \tag{1}$$

where S_p is the area of the image of the particle, S_4 is the area of the largest 4-sided polygon (generally a trapezoid) that contacts the perimeter of the particle and 0.5708 is a numerical factor that normalizes S so that it varies between 0 for a square (cube) and 1 for a circle (sphere). The parameter Σ adequately captures the flatness of the interfaces and is independent of A. Measurements of A and S were made from scanned and enlarged dark-field electron micrographs using

the Image-Pro Plus^{TM} software package. Depending on the type of specimen and aging condition the dimensions of between 300 and 600 particles were typically measured, though this number was as large as 1000 for particles in some RC specimens.

As the stress increases precipitates of a given size generally tend to become more non-equiaxed and their interfaces are more planar, though this depends on the γ' volume fraction. The applied compressive stress also promotes the coalescence of γ' precipitates. This tendency is more pronounced the higher the γ' volume fraction and appears to be its main influence on directional coarsening during elastic deformation.

IV.2 Ni-Ge Single Crystals Aged Under Compression (N. Starostina and S.V. Prikhodko)

The results of this research were published in paper #5, Sec. II. A summary of the main results follows.

The kinetics of coarsening of Ni_3Ge precipitates under applied compressive stress were investigated in [100]-oriented monocrystalline Ni-Ge alloy specimens (nominal composition 12.92 ± 0.5 at. % Ge) aged at 625 °C. The maximum stress used was ~100 MPa, and the strains were predominantly elastic (plastic deformation was less than 1% except for the largest stress, where it was 3%). The microstructures were examined by TEM of the (100) sections cut perpendicular to the applied stress.

The alloy with a nominal composition of 12.92 at. % Ge was first prepared by arc-melting buttons weighing 30-50 g from high-purity (99.99% Ni, 99.999% Ge) starting materials. The buttons were cut into small pieces, placed in a small, flat-bottomed alumina crucible, melted inside a vacuum furnace under a pressure of 10^{-5} torr and slowly cooled at 3 °C/h through the melting range, yielding a bulk polycrystalline sample with a few large grains exceeding 10 mm in size. The weight losses during arc-melting and vacuum furnace re-melting were very small. Single-crystal specimens with maximum dimensions of ~3 mm in dia. and ~4 mm in length were oriented and cut from the larger grains. Other specimens were smaller than this, but large enough to test. The crystals were oriented parallel to [100] using the Laue back-reflection method. The deviation from [100] did not exceed 2°. A total of 14 specimens, cylindrical in shape, were prepared. One single crystal grain produced 4 cylindrical specimens with diameters $\langle d \rangle = 2.98 \pm 0.01$ mm, and length $\langle \ell \rangle = 3.7 \pm 0.1$ mm. Another single crystal grain yielded 9 cylindrical specimens with $\langle d \rangle = 2.53 \pm 0.01$ mm and $\langle \ell \rangle$ ranging from 0.8 to 2.4 mm; one additional specimen from this crystal was obtained with $\langle d \rangle = 1.577 \pm 0.008$ mm, $\langle \ell \rangle = 0.833 \pm 0.001$. For the chosen aging temperature, 625 °C, the average volume fraction of γ' in the Ni-Ge alloys was estimated to be 0.14, using the most recent phase boundaries in the Ni-Ni_3Ge alloy system.

The cylindrical specimens were cut from the selected big grains of the bulk sample using elecrtic-spark discharge machining (EDM). Prior to testing they were electrochemically polished using a solution of H_2SO_4 and CH_3OH (to remove traces of Cu due to the copper wire used in EDM) and solution treated at 1150 °C for 45 min followed by quenching into refrigerated brine. The specimens were aged for 48, 144 or 288 h under applied compressive stresses in the range 6 to ~100 MPa. Unstressed reference specimens, made from cold-rolled and solution-treated sheet taken from the same alloy used to grow the single crystals, were placed adjacent to the compression tested specimens. The small compression specimens used in this work essentially minimized or eliminated possible temperature gradients along their length, as well as temperature differences between the compression and reference specimens.

The specimens were aged under compressive stress using the same stainless steel fixture in the work on Ni-Al alloys. The applied stresses were chosen to limit the extent of plastic deformation during aging. The plastic strain was measured for each compressed cylinder; it was less than 1% for the longest aging time under a stress of 48 MPa. For the highest stress used, ~100 MPa, we observed a plastic strain of about 3% after 48 h. For this reason the specimen aged for

144 h at 100 MPa was pre-aged for 6 h prior to applying the load. This undoubtedly resulted in a small increase in the average size of the precipitates, but limited the plastic strain to less than 1%. Temperature control was maintained to within ± 2 °C. A protective argon atmosphere prevented oxidation of the specimens and fixture during testing. Samples for transmission electron microscopy were prepared and examined using the same conditions as for the Ni-Al alloys.

The effects of applied stress are small, but conclusive. Compressive stress retards the kinetics of coarsening, tends to make the precipitates more spherical in shape and reduces their aspect ratio. The elastic anisotropy of Ni_3Al is greater than that of Ni_3Ge, and it is suggested that this parameter influences the shape during coarsening, even though it is not included in treatments of elastic interactions among precipitates.

IV.3 Ni-Ga Single Crystals Aged Under Compression (N. Starostina)

Twenty single crystal specimens, cylindrical in shape, were prepared from slices of a single crystal grown by the Bridgman method at the Alloy Preparation Laboratory, Ames, IA. As in the other work, the slices were oriented parallel to (001) using the Laue back-reflection method and the deviation did not exceed 2°. All the cylinders had approximately the same diameter and length, 3.00 ± 0.01 and 3.60 ± 0.01 mm, respectively. The compositions of the slices were checked with the help of Curie temperature measurements. A strong composition gradient was found along the length of the crystal, so the composition of every individual cylinder was accurately checked using Energy-Dispersive X-Ray Spectroscopy (EDS) and magnetic analysis. The composition varied from 14.71 to 20.19 at. % Ga over a length of about 25 mm.

Selected cylindrical specimens with comparable compositions were solution treated at 1220 °C for 45 min, quenched into brine and aged for 2, 4 or 8 h under applied stresses in the range 0 to 150 MPa at 650 °C. The volume fraction of Ni_3Ga in these specimens was estimated to lie between 0.22 and 0.26. The specimens were aged under stress in the same apparatus used for the other experiments. Plastic strain was measured for each specimen and was found not to exceed 1% at the highest stress (150 MPa) even for the longest aging time. The composition of every single TEM sample was carefully double-checked by EDS. Additionally, the compositions of 2 TEM disks were also examined by Induced Coupled Plasma (ICP) chemical analysis, which is a technique capable of measuring chemical composition with high accuracy. The composition measured using ICP was in very good agreement with the results of the EDS measurements.

Representative precipitate microstructures in specimens aged for 8 h under zero applied stress and an applied stress of 50 MPa are shown in Fig. 1. The precipitates in the specimen aged under applied stress are visibly smaller. The data on average particle size as a function of applied stress are shown in Fig. 2. Low stresses markedly affect the kinetics of coarsening, which apparently pass through a minimum, resembling to some extent the behavior observed for Ni_3Al precipitates. The results shown in Fig. 3, where $\langle r \rangle^3$ is plotted vs. t, are also consistent with a minimum coarsening rate at intermediate stresses. A linear relationship between $\langle r \rangle^3$ and t is not well obeyed, but if the data are taken at face value the rate constant k would pass through a minimum at small stresses. At higher stresses the kinetics are faster, but still remain slower than they are under stress-free conditions. The dependencies of Σ and A on σ are shown in Fig. 4. The shape remains unaffected by the stress, while the aspect ratio decreases considerably at small stresses, but remains nearly constant at the higher stresses.

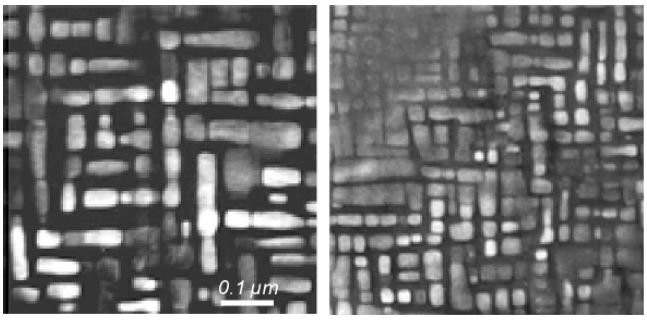

(a) (b)

Figure 1. Ni_3Ga precipitate microstructures in specimens aged for 8 h under stress-free conditions (a) and an applied stress of 50 MPa (b) at 650 °C.

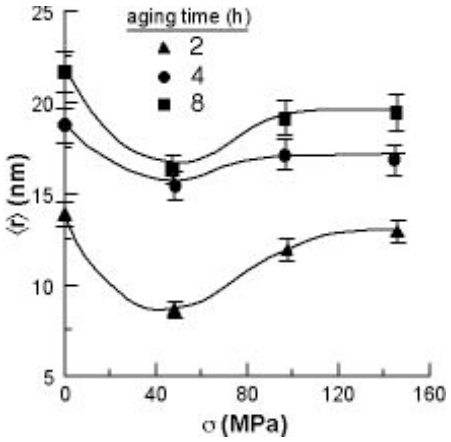

Figure 2. Variation of the average Ni_3Ga particle radius with applied stress for the 3 aging times used in this investigation.

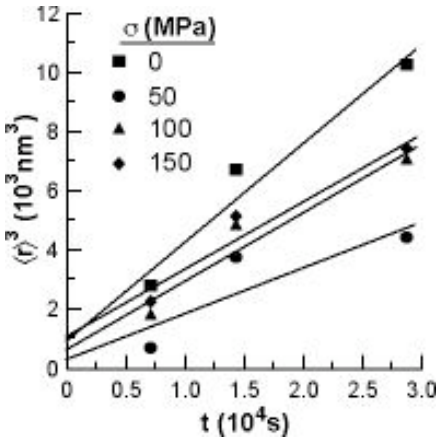

Figure 3. The dependence of the cube of the average Ni_3Ga precipitate radius on aging time under applied stress.

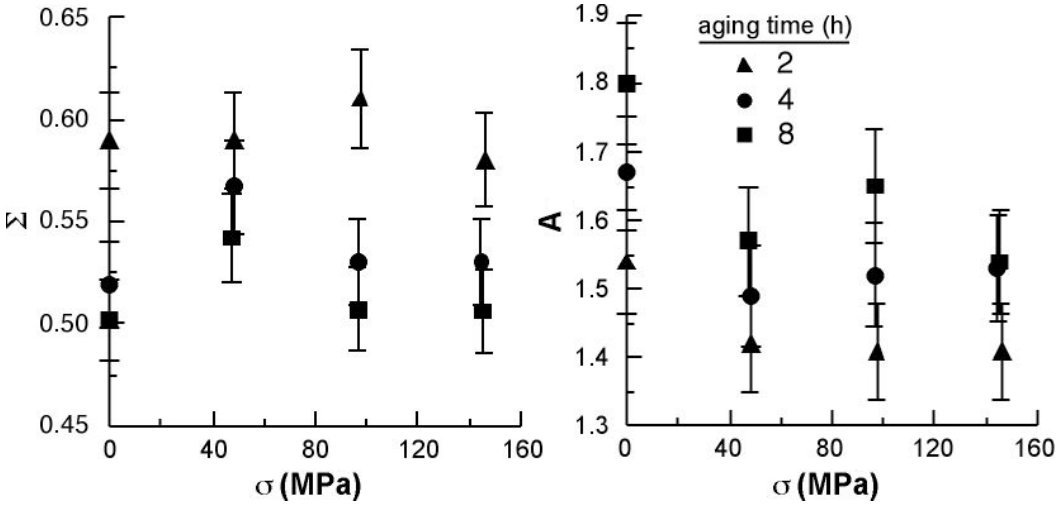

(a) (b)

Figure 4. The dependence of the shape parameter, Σ, and Aspect ratio, A, on the average size of Ni_3Ga precipitates for different applied stresses.

IV.4 Ni-Si Single Crystals Aged Under Compression (N. Starostina and D. Detch)

Fifteen cylinders 3 mm in diameter and approximately 1.4 mm in height were previously cut from a cylinder of a [001]-oriented Ni-Si alloy with a nominal composition of 11.4 at. % Si. The compositions of the 3 mm samples were originally determined using energy-dispersive spectroscopy (EDS) in our scanning electron microscope (SEM). Due to uncertainties in the results obtained by EDS the compositions of the individual specimens need to be double-checked using magnetic measurements of their ferromagnetic Curie temperatures. This step is necessary because of the large concentration gradients in the original single crystals purchased several years ago from the Alloy Preparation Laboratory. Specimens were aged at 625 °C for 24, 120, 360 and 504 h under stresses of 25, 50 and 130 MPa, but only a few were examined by TEM. The Ni_3Si precipitate microstructure in a sample aged for 24 h under a stress of 50 MPa is shown in Fig. 5. The average sizes and size distribution were not measured, but it is evident that the shapes of the precipitates are nearly spherical, as expected from the results of numerous experiments on the aging of Ni-Si alloys under stress-free conditions. Unfortunately, Ms. Detch, who took over the project from Ms. Starostina, left UCLA before completing the work.

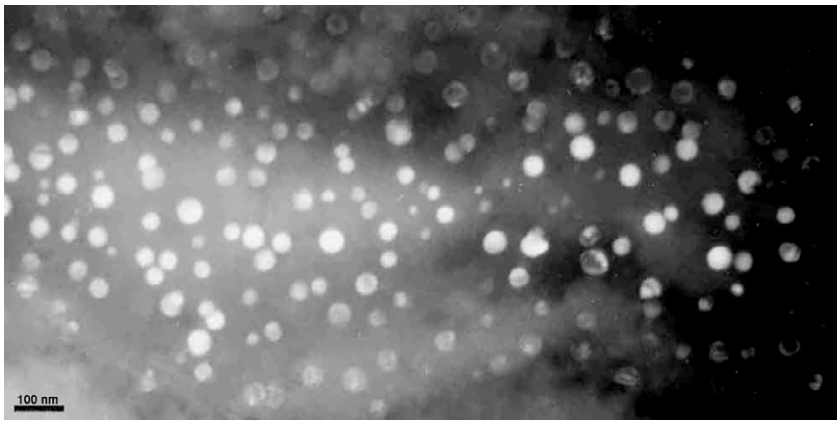

Figure 5. Dark-field TEM photo of the Ni_3Si precipitates in the specimen aged for 24 h under an applied stress of 50 MPa.

IV.5 Ni-Al Single Crystals Aged Under Tension (R. Guerrero)

A single-crystal Ni-Al alloy containing 13.4 at. % Al was used in all the experiments. It was grown by the Bridgman method and purchased from the Alloy Preparation Laboratory, Ames, IA. Slices in (100) orientation were cut from the single crystal and cylinders were subsequently cut from the slices using EDM. In all cases the crystals were oriented using the Laue back-reflection x-ray method. The initial experiments on aging tapered specimens with threaded ends under applied stress were unsuccessful because the stresses used were too large. All specimens subjected to stresses larger than 60 MPa failed, hence this was the maximum stress used in the experiments. Experiments were conducted on tapered and cylindrical specimens in 2 different furnaces. The tapered specimens are shown schematically in Fig. 6. The cylindrical specimens were approximately the same length as tapered ones, but their gage sections were ~3 mm in diameter.

Two furnaces were used to age the specimens under applied tensile loading. The tapered specimens were aged in a water-cooled radiant heating furnace with 4 heating elements. It is shown in Fig. 7 in the open position with the heating lamps visible.

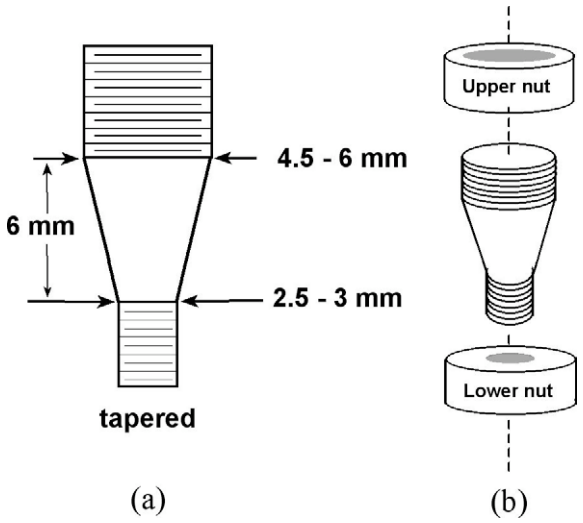

Figure 6. Schematic diagrams of the tensile specimen configurations used in this research project: (a) Tapered specimen; (b) Illustrating the circular upper and lower nuts screwed onto the tops and bottoms of the specimens.

The specimen and tensile fixture were contained inside a quartz tube and protected from oxidation by an atmosphere of high-purity Ar gas. The tensile load was applied via a lever arm to the linkage rod that passes through a sliding vacuum seal into the quartz tube, where it is attached to the upper plate of the tensile fixture. The average heating rate from room temperature to 640 °C was 0.5 °C/s; it takes about a minute to cool from 640 to ~500 °C. The tensile loading fixture is visible in the center of the furnace and is shown schematically, and in greater detail, in Fig. 8. In Fig. 8(a) only 2 of the 3 stationary stainless steel rods, R, that are attached to the frame of the test apparatus, are shown. The load is transmitted to the specimen via the linkage rod labeled L, which is attached to the upper plate of the tensile fixture. The specimen enters the fixture via slots in the upper and lower guide plates which make contact with the upper and lower nuts screwed onto the ends of the specimen. The measuring thermocouple is maintained in close proximity to the specimen. A photograph of the tensile fixture, with a dummy tapered stainless steel specimen inserted, is shown in Fig. 8(b). Not shown in the figure is a layer of Pt mesh surrounding the specimen. Its purpose is to help reduce a possible longitudinal temperature gradient along the length of the specimen. The differences in temperature along the length of the specimens were measured to be less than 0.2 °C.

The furnace and configuration used to test the cylindrical specimens is shown in Fig. 9. In this furnace the load is applied directly to the specimens, and since the temperature is constant over a distance of about 100 mm several specimens can be tested at the same time; the arrangement for testing 5 specimens is also shown in Fig. 9. A typical testing sequence involves testing the "chain" of specimens for a specific aging time, air-cooling them all to room temperature, removing 1 specimen for examination by TEM, then re-inserting the remaining ones for another aging time, and repeating this process until the last specimen is aged for the maximum aging time. During all the aging steps the specimens are protected by an Ar atmosphere.

Figure 7. Photograph of the new apparatus for aging specimens under stress. The hinged furnace is open, exposing the heating lamps and tensile loading fixture. Part of the linkage rod, L, outside the furnace and atmosphere chamber is visible.

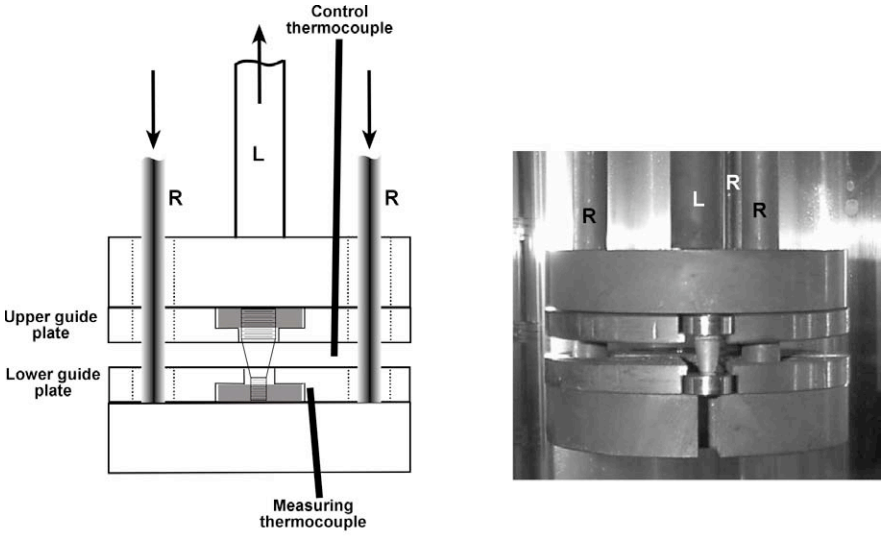

(a) (b)

Figure 8. (a) Schematic diagram of the tensile loading fixture, illustrating the positions of the thermocouples, rods attached to the loading frame (R), and the linkage rod (L) through which the load is applied. (b) A photograph of the tensile loading fixture with a dummy stainless steel specimen in place.

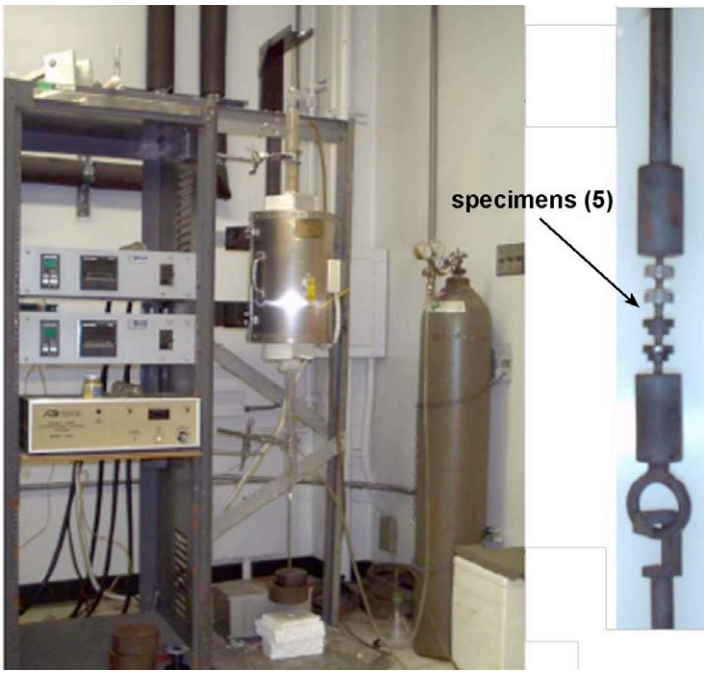

Figure 9. Photograph of the resistive heating furnace used to age cylindrical Ni-Al specimens under applied tensile stress. The loading fixture containing 5 tensile specimens is also shown.

Specimens for TEM were prepared from the tensile specimens in the usual way, i.e. by cutting slices at selected points along the length normal to the axis of the applied stress. This method introduces an uncertainty into the precise value of the stress when tapered specimens are used, but the uncertainty is small and manageable, about ± 5 MPa. A few specimens were tested and examined in a (001) section parallel to the axis of the applied stress. The sizes, shapes and aspect ratios were measured using the same procedures applied to all the alloys in this research program.

Data on the kinetics of coarsening are shown in Fig. 10, where $\langle r \rangle^3$ is plotted vs. aging time for applied stresses up to 60 MPa. The linearity of the plots is quite good and it is apparent that the rate constant for coarsening increases with applied stress up to 45 MPa, then evidently decreases at the 2 larger stresses. In an attempt to rationalize these results a series of aging experiments were conducted under applied stress in which the microstructures were examined in the (001) section parallel to the applied stress. Typical γ' microstructures in sections normal and parallel to the stress axis are shown in Fig. 11. It is apparent in Fig. 11(b) that the shapes of the precipitates are elongated in the direction of the applied stress. The rate constant, k, is plotted vs. σ in Fig. 12. The point P indicates the value of k obtained from the specimens cut parallel to the applied stress. This datum suggests that the tendency for k to increase with σ continues provided that the sizes of the precipitates are measured in the parallel section. At present there is no satisfactory explanation for this behavior.

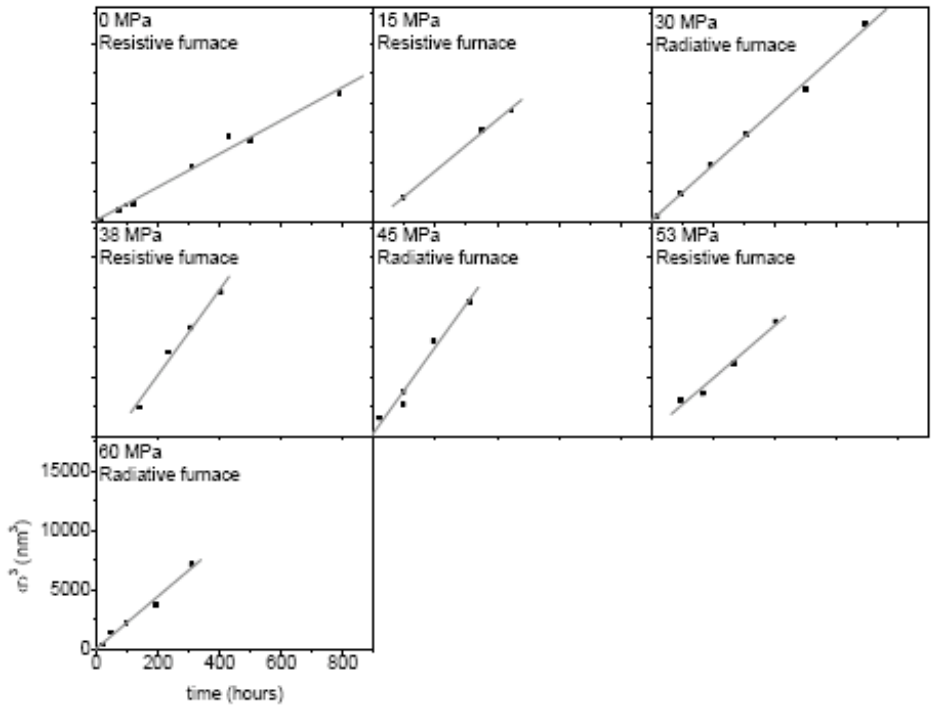

Figure 10. Plots of the cube of the average precipitate "radius" vs.aging time for specimens tested under applied tensile stress at 640 °C. The least-squares fits to the curves were used to determine the rate-constants, k, from the slopes.

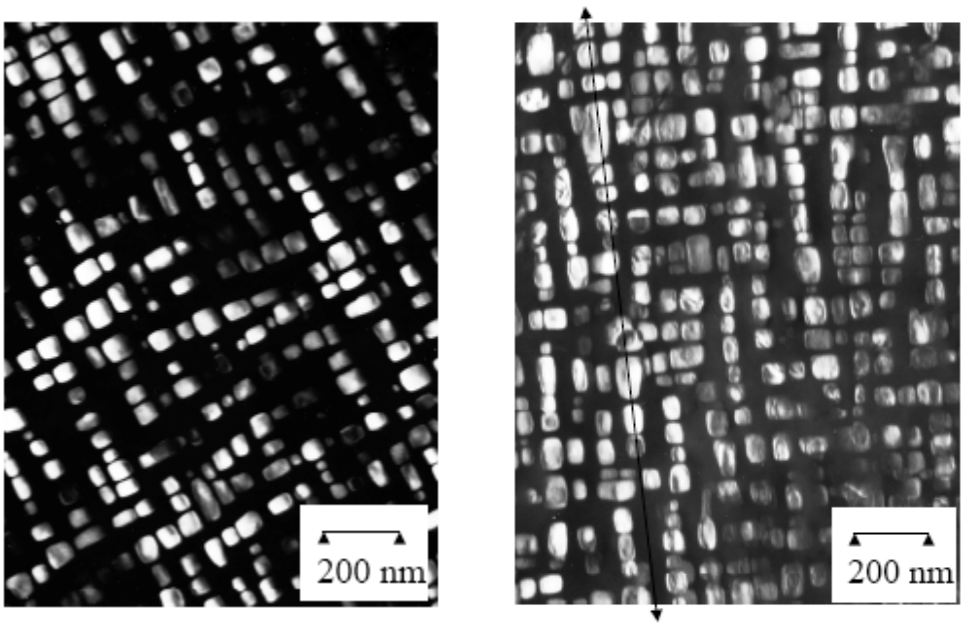

(a) (b)

Figure 11. Dark-field TEM images of the γ′ precipitate microstructures in a specimen aged for 404 h at 640 °C under a tensile stress of 53 MPa. The specimen in (a) is from a slice normal to the axis of σ, while the specimen in (b) shows the precipitates in the (001) plane containing the axis of the applied stress, which is indicated by the arrows.

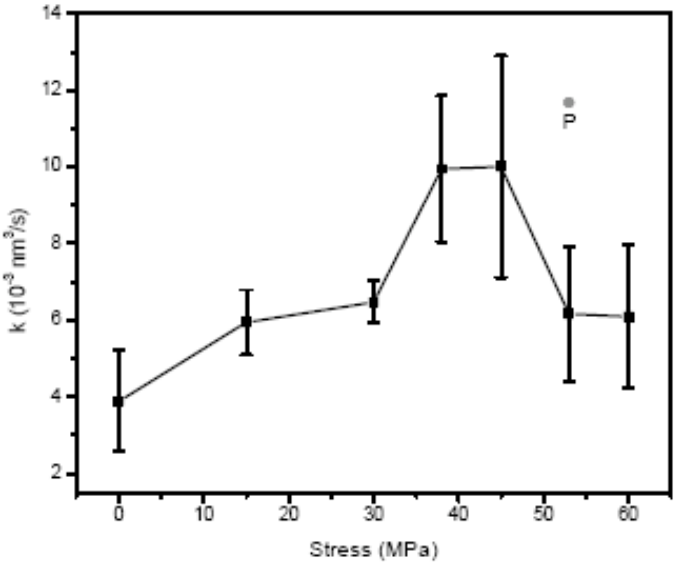

Figure 12. The dependence of the rate constant for coarsening, k, on applied stress. All the data are from TEM micrographs of the γ' precipitate microstructures normal to the axis of the applied stress. The point P is taken from measurements on specimens cut parallel to (001) containing the axis of the applied stress.

Measurements were made of the shape parameter, Σ, and aspect ratio, A. Data on the behavior of the precipitates in the cylindrical specimens are shown in Figs. 13 and 14. There is a slight tendency for Σ to increase as the stress increases for particles of a given size, but within the limits of experimental error Σ is nearly constant. Examination of the data taken from tapered specimens showed a similar trend, but the values of Σ were slightly larger, suggesting that the precipitates were slightly more spherical in shape. The open circles in Fig. 12 represent data from specimens cut parallel to the axis of the applied stress; these precipitates were consistently more cuboidal in shape than in sections normal to the applied stress.

The aspect ratios in the cylindrical specimens (Fig. 14) were also nearly constant with applied stress for particles of a given size. The dependencies of A on σ in the tapered specimens were similar to those seen in Fig. 14. As of this writing the analysis of all the data taken on the specimens aged under applied tensile stress is incomplete, but it is anticipated that the results will be analyzed and published in the near future.

IV.6 Measurements of the Elastic Constants of Ni-Si, Ni-Ga and Ni-Ge Alloys (D.G. Isaak, S.V. Prikhodko, J.D. Carnes, S. Moser, Y. Ma and N. Starostina)

The results of this research were published in papers #1 and 6, Sec. II. A summary of the main results follows.

The adiabatic elastic stiffness constants C_{ij} of Ni-Si single-crystal solid-solution alloys of two slightly different compositions, 10.78 and 11.17 at. % Si, were measured over the temperature range from 20 to 900 °C using the rectangular parallelepiped resonance (RPR) method. The isotropic elastic constants of the polycrystalline ordered intermetallic compound Ni_3Si containing 23 at. % Si were also measured over this temperature range. Values of the C_{ij} for Ni_3Si were estimated from the data on the polycrystalline alloy, as well as from published data in the literature on isomorphous ternary ordered intermetallic compounds containing different amounts of Si.

Using measured values and previously published data, the stiffness constants of Ni_3Ti were also estimated; these are the only available data on this alloy. The estimated single crystal elastic constants of Ni_3Si, as well as the experimentally measured bulk modulus, are considerably smaller than published values calculated from first-principles methods. The same is true for the C_{ij} of Ni_3Ti, but the discrepancies are smaller.

The C_{ij} for fcc single-crystal specimens of Ni-12.16 at.% Ga and Ni-11.59 at.% Ge were measured using the same method as that employed for the Ni-Si alloys. We estimated the values of the parameter ΔC^* for both the Ni-Ga and Ni-Ge systems using the data on the C_{ij} solid solutions along with literature data on the elastic constants of Ni_3Ga and Ni_3Ge; $\Delta C^* = \Delta C_{11} - \Delta C_{12}$, which represent the differences between C_{11} and C_{12} of the ordered phases and disordered solid solutions, respectively. We find that the value of the ΔC^* parameter for Ni-Ge alloy is the largest among all studied Ni-base alloys. The large positive value of ΔC^* could possibly account for the observation that cuboidal-shaped Ni_3Ge precipitates *never* coalesce, despite the obviously stong elastic interactions among them that lead to alignment along ⟨100⟩.

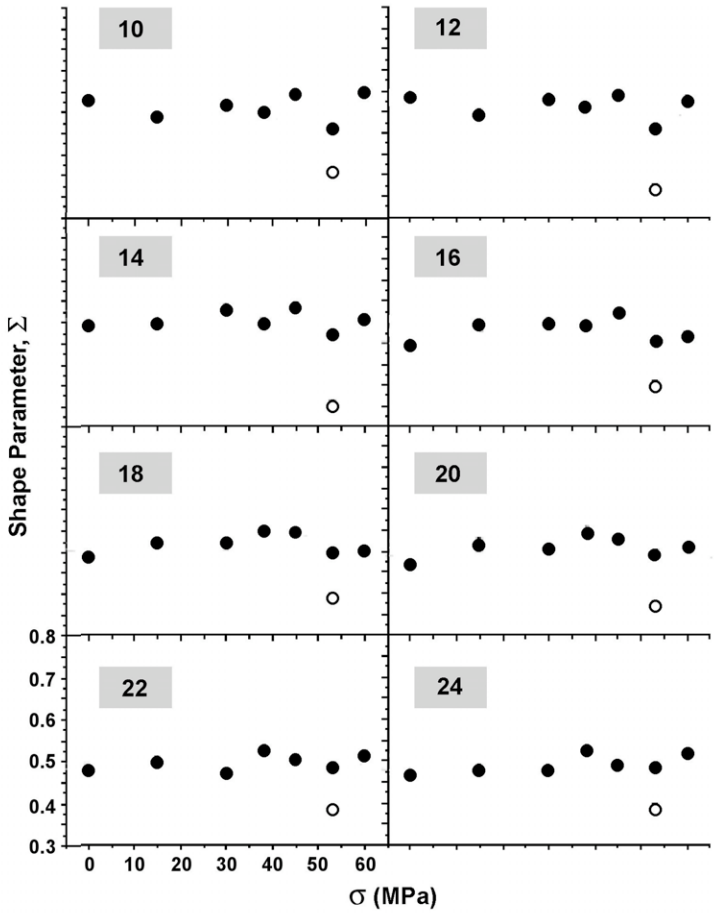

Figure 13. The dependence of the shape parameter, Σ, on applied stress, σ, for precipitates of the same "radius", the values of which are inset in each figure. The filled circles represent data from samples cut normal to the axis of the applied stress and the open circles represent data from a specimen cut parallel to (001), containing the axis of the applied stress.

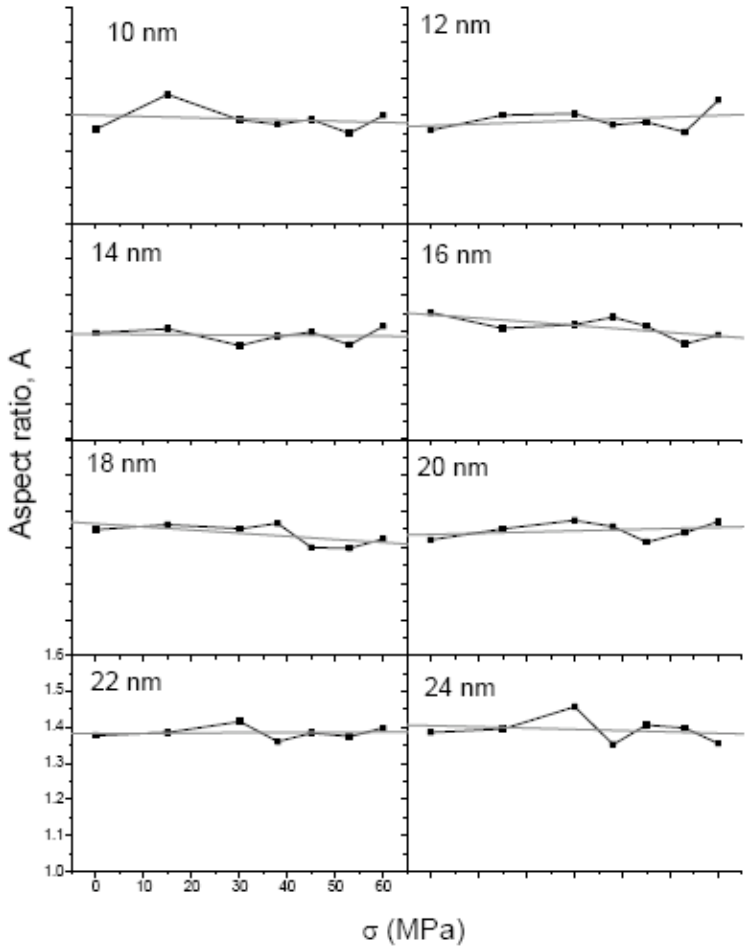

Figure 14. The dependence of the aspect ratio, A, on applied stress, σ, for precipitates of the same "radius", the values of which are inset in each figure. The data are all from samples cut normal to the axis of the applied stress.